Chemical Physics 174 (1993) 267–276
North-Holland

High-resolution laser-induced fluorescence study of a cage molecule, 1,4-diazabicyclo[2,2,2]octane, DABCO

D. Consalvo, M. Drabbels, G. Berden, W. Leo Meerts, D.H. Parker and J. Reuss
Molecular and Laser Physics, University of Nijmegen, Toernooiveld, 6525 ED Nijmegen, The Netherlands

Received 3 March 1993

Rotationally resolved laser-induced fluorescence spectra of the caged amine DABCO (1,4-diazabicyclo[2,2,2]octane) seeded in a supersonic He beam are recorded using a high-resolution pulsed dye laser system. Both one-photon and two-photon spectra of the $S_1(A_1')\leftarrow S_0(A_1')$ transition are measured. In the one-photon spectra we observe electric quadrupole transitions to the S_1 origin and to a_1' vibrational levels and vibrationally induced electric dipole transitions to a_2'' and e' vibrational levels. For the first time parallel one-photon transitions with their characteristic rotational structure have been observed. Rotational constants are extracted from both the two-photon and one-photon spectra. The quantum mechanical model previously applied to explain the occurrence of the "memory effect" in fluorescence spectra emanating from the $S_1(e')$ levels is extended here for the $S_1(a_2'')$ levels. Despite the presence of long progressions in several vibrational modes for the $S_1(A_1')\leftarrow S_0(A_1')$ transition, the difference in S_0 and S_1 rotational constants are remarkably small, suggesting that compensating geometry changes take place on excitation to S_1.

1. Introduction

In the past much effort has been devoted to investigation of the vibrational structure of the 1,4-diazabicyclo[2,2,2]octane molecule, DABCO, a highly symmetric amine which belongs to the molecular point group D_{3h}. No high-resolution excitation spectra have been reported up to now which would clarify ambiguous assignments and/or confirm previous findings based upon low-resolution electronic spectra [1,2]. From the rotational structure observed in the experiment here reported conclusions can be drawn with respect to the symmetry of the vibrational levels involved. Since the DABCO molecule does not possess a permanent dipole moment no information on the geometrical structure can be obtained by microwave spectroscopy. In the present study high-resolution laser-induced fluorescence (LIF) spectroscopy is applied to mode characterization. Additional information concerning the change of geometrical structure upon electronic excitation is obtained.

Transitions from the totally symmetric electronic ground state, S_0, to the first electronically excited state, S_1, which is also totally symmetric, are one-photon forbidden and two-photon allowed. The forbidden transition becomes partially allowed through an admixture of the nearby S_2 state, of E' symmetry, and of another excited state of A_2'' symmetry, to the S_1 state of A_1' symmetry. Therefore both one- and two-photon spectra are useful to gain insight into symmetry of the active vibrational modes.

The electronic structure and the orbital ordering have been investigated previously [3–5]. The highest filled molecular orbital (HOMO) was found to be the plus combination of lone-pairs, with the minus combination lying almost 2 eV lower in energy. All of the DABCO electronically excited states are Rydberg states in nature, with $(3s)S_1(A_1')$ at 35783 cm^{-1} and $(3p_{xy})S_2(E')$ at 39814 cm^{-1}.

2. Experimental

The experimental setup has been described in detail before [6]. A molecular beam is formed by expanding DABCO (vapor pressure 0.4 Torr at room temperature) seeded in 1.5 atm He or N_2 through a pulsed valve with an orifice with a diameter of 1 mm. No significant preferential orientation of the DABCO

molecule in the molecular beam is expected. An unfocused laser beam, 5 mm diameter, crosses the molecular beam perpendicularly 45 mm downstream of the nozzle and induces, via one- or two-photon absorption, the $S_1 \leftarrow S_0$ transition in DABCO. For one-photon (two-photon) excitation the polarization of the laser beam is parallel (perpendicular) to the molecular beam axis.

To rotationally resolve the LIF excitation spectrum of DABCO a laser source with high peak power and narrow bandwidth is used. Radiation from a cw ring dye laser (Spectra Physics, 380D) operating on Rhodamine 110 dye is amplified in a home built four-stage pulsed dye amplifier (PDA) system operating on fluorescein 27 dye. The PDA system is pumped by a frequency-doubled Q-switched Nd:YAG laser (Quantel YG 681C-10), producing a laser beam with a pulse energy of 100 mJ and a bandwidth of 135 MHz. For one-photon experiments this radiation is frequency doubled in a KDP crystal yielding 20 mJ of UV light. For absolute frequency calibration the I_2 absorption spectrum is recorded simultaneously with the excitation spectrum. For relative frequency calibration the transmission peaks of a temperature and pressure stabilized interferometer with a free spectra range of 299.41 MHz are recorded.

The laser-induced fluorescence is collected from a 3 mm diameter probe region by a quartz lens system and imaged onto a photomultiplier. In order to reduce the scattered light in the two-photon experiments a Schott UG 11 filter is placed in front of the photomultiplier. The signals are processed by a digital oscilloscope (LeCroy 7400) and a boxcar averager (SRS 250) interfaced with a Personal Computer. The linewidth observed in the experiments is almost completely determined by the residual Doppler broadening of the molecular beam and amounts to 400 and 700 MHz for N_2 and He as seeding gas, respectively. The rotational temperature is found to be 1 K for He and 7 K for N_2. When argon is used as seeding gas no excitation spectra of DABCO could be observed probably due to massive cluster formation [7].

3. Theoretical aspects

Transitions to the first electronically excited state can be induced by one- and two-photon processes obeying different selection rules [8]. An overview is given in table 1, where the possible transitions to the S_1 state are summarized according to the multiplication rules of D_{3h}.

By one-photon excitation only levels of e′ and a_2'' symmetry can be probed, whereas two-photon transitions involve final states of a_1' symmetry. In case of a quadrupole one-photon transition the two-photon selection rules hold.

In a prolate symmetric top molecule like DABCO the transition energy for an excitation from a nondegenerate state to a degenerate state, i.e. for an $e' \leftarrow a_1'$ transition is given by [9]

$$\begin{aligned}\Delta E_{\mathrm{rot}} &= \nu_0 + B'J'(J'+1) - B''J''(J''+1) \\ &+ [A'(1-2\zeta) - B'] \\ &\pm 2[A'(1-\zeta) - B']K \\ &+ [(A'-B') - (A''-B'')]K^2 . \end{aligned} \tag{1}$$

The upper (lower) sign has to be taken for $\Delta K = +1$ (-1) transitions. In the equation above J'' and K are the rotational quantum numbers and A'' and B'' the rotational constants for the ground state (J' for the final state). The transition takes place between levels

Table 1
Selection rules for the measured transitions. The two-photon selection rules are derived from the multiplication rules: $e' \otimes e' = a_1' + e'$ and $a_2'' \otimes a_2'' = a_1'$

		Selection rules	
		vibrational	rotational
$1h\nu$	$a_1' \rightarrow e'$ dipole transition	$(\perp)$	$\lvert\Delta J\rvert = 0, 1$ $\lvert\Delta K\rvert = 1$
	$a_1' \rightarrow a_2''$ dipole transition	$(\parallel)$	$\lvert\Delta J\rvert = 0, 1$ $\lvert\Delta K\rvert = 0$
	$a_1' \rightarrow a_1'$ quadrupole transition		$\lvert\Delta J\rvert = 0, 1, 2$ $\lvert\Delta K\rvert = 0$ $J=0 \nleftrightarrow J=0$ $J=1 \nleftrightarrow J=0$
$2h\nu$	$a_1' \rightarrow a_1'$ $2\times$dipole transition		$\lvert\Delta J\rvert = 0, 1, 2$ $\lvert\Delta K\rvert = 0$ $J=0 \nleftrightarrow J=0$ $J=1 \nleftrightarrow J=0$

of which one is degenerate; as a consequence the Coriolis coupling (ζ) and l-doubling terms have to be included in the expression for the level energy. The l-doubling is here neglected because in the measured spectra no irregularities for the $K'=1$ levels have been found which normally are taken as evidence of l-doubling [9].

For these perpendicular transitions it is readily seen that while the B constant can be determined for the ground and for the excited state, only the difference between the ground state and the excited state value can be quantified for the A constant, see table 2.

For an excitation from a nondegenerate state to a nondegenerate state, i.e. for an $a_2'' \leftarrow a_1'$ or for an $a_1' \leftarrow a_1'$ type of transition eq. (1) becomes [9]

$$\Delta E_{\mathrm{rot}} = \nu_0 + B'J'(J'+1) - B''J''(J''+1) + [(A'-B') - (A''-B'')]K^2 . \quad (2)$$

For a parallel dipole transition $|\Delta J| = 0, 1$ and for a quadrupole transition $|\Delta J| = 0, 1, 2$; the condition $\Delta K = 0$ is valid for both. From the selection rules for a quadrupole transition an alternation of intensity (in fact $|\Delta J| = 2$ transitions overlap with every second $|\Delta J| = 1$) is expected.

From the fit of the experimental data to eq. (1) the following five parameters are obtained: the rotational constants B'' and B' for the ground and for the excited state, the rotational constant A' in combination with the Coriolis parameter, $A'(1-\zeta)$, the change of the rotational constant upon excitation, $A'-A''$, and the effective band origin $\nu_x' + A'(1-2\zeta)B'$, see table 2. The real band origin can be estimated within 6 GHz, see table 3.

For dipole transition the intensities are given by the following expression:

$$I = C_\nu A_{KJ} g_{KJ} \exp(-E_{\mathrm{rot}}/kT) , \quad (3)$$

where A_{KJ} are the Hönl–London factors [9]. The intensities of single rotational lines in the LIF spectrum, assuming a Boltzmann distribution, are essentially determined by the Hönl–London factors; the omission of the Hönl–London factors did not lead to an acceptable fit.

The intensity of two-photon transitions with $\Delta J = \Delta K = 0$ is given by a sum of two terms, as is fully outlined in ref. [8]. For a quadrupole transition one of the two contributions disappears, which explains the lower relative intensity of the Q-branch with respect to the two-photon case. In our spectra we encounter two photon transitions and quadrupole transitions for the same initial and final states, e.g. for the 0_0^0 band. The quadrupole intensity of the Q branch is much weaker, i.e. the vanishing term gives the dominant contribution.

In these intensity considerations, the influence of spin statistics, g_{KJ} in eq. (3), has been neglected. The twelve equivalent hydrogen spins are assumed to yield a small difference in weight factors, a conjecture sustained by the good intensity fit obtained for our data (better than 10%).

Structural data related to the solid phase of DABCO [4] can be used for comparison. The interatomic distances from ref. [4] are assumed fixed and the appropriate geometry is chosen to be tetrahedral for all the angles. A calculation has been performed to determine the rotational constants in the ground state. The molecule is a prolate, nearly spherical top, if the NCC angle (α) is tetrahedral. From the calculation performed varying α follows that a spherical top would require 105° for α at equilibrium, while the molecule would be an oblate top for $\alpha \leqslant 105°$. The

Table 2
Molecular constants (in MHz) of some of the observed transitions. The band origins (in cm^{-1}) are given with respect to the 0_0^0 transition at 35783.234 cm^{-1}. The error in these values is 0.005 cm^{-1}. For the perpendicular transitions, 26_0^1 and 27_0^1, the effective band origin is given.

	0_0^0	$9_0^1 13_1^0$	26_0^1	27_0^1
B''	2509.8(2.8)	2464.5(5.8)	2509.8(2.8)	2509.8(2.8)
ΔB	0.6(0.6)	1.4(0.6)	0.2(2.6)	0.3(2.9)
ΔA	1.6(1.8)	1.5(1.8)	12.7(1.1)	17.6(0.7)
$A'(1-\zeta)$	–	–	3065.9(1.3)	4030.7(1.2)
ν_0	0	689.506	825.162	449.113

Table 3
Observed rovibronic $S_1 \leftarrow S_0$ transitions. Rotationally resolved parallel and perpendicular transitions are indicated by ∥ and ⊥, respectively. Quadrupole transitions are labelled by Q. The band origins are given with respect to the 0_0^0 transition at 35783.234 cm^{-1}. Isotope shifts are indicated by $\Delta^{13}C$ and $\Delta^{15}N$. Band origins and isotope shifts are given in cm^{-1}. The error in the observed frequencies is 0.005 cm^{-1}. Fundamentals are underlined

Frequency	One-photon	Two-photon	Symmetry	Assign.	Remarks
0	Q	∥	a_1'	0_0^0	$\Delta^{15}N=-1.571$, $\Delta^{13}C=+2.535$ [a], fig. 2
203.762	?	∥	$?+a_1'$	13_0^2	one-photon weak and structureless
205.56	?	–	?	?	weak and structureless
449.113	⊥	–	e′	27_0^1	fig. 3a
670.844	–	∥	a_1'	6_0^1	$\Delta^{15}N=-1.632$, $\Delta^{13}C=-1.489$
671.479	∥	–	a_2''	$27_0^1+36_0^1$	weak
689.506	∥	–	a_2''	$9_0^1 13_1^0$	hot band transition, see table 2 for B″
691.152	–	∥	a_1'	36_0^2	weak
777.605	Q	∥	a_1'	5_0^1	
825.162	⊥	–	e′	26_0^1	fig. 3b
882.189	Q	∥	a_1'	4_0^1	
883.080	∥	–	a_2''	$9_0^1+13_0^1$	weak
897.391	⊥	∥	$e'+a_1'$	27_0^2,	two-photon weak
900.51	⊥	–	e′	25_0^1,	weak
901.070	–	∥	a_1'	$35_0^1+36_0^1$	
919.467	∥	–	a_2''	17_0^1	$\Delta^{15}N=-0.945$, $\Delta^{13}C=-1.891$, fig. 4
1011.267	⊥	–	e′	24_0^1	

[a] Two additional isotopomers are observed shifted by $\Delta(^{13}C\ ^{15}N)=+1.605\ cm^{-1}$ and $\Delta(^{13}C)^2=+1.893\ cm^{-1}$.

structure [4] allows to calculate the rotational spectrum once an assumption on the excited state parameters has been made.

Next we discuss the shifts of the band origin arising from isotopic substitution. For the 0_0^0 band this shift represents the cumulative zero-point effect of isotopic replacement on the 36 vibrational modes. For each mode the amplitude of the motion changes upon isotopic substitution; moreover the motion itself will be modified by symmetry breaking. The two effects are combined and give origin to the observed shifts $\Delta^{13}C$ and $\Delta^{15}N$ discussed in this context.

For illustration we restrict the discussion to a situation where either the q_{C-C} or q_{C-N} stretch dominates. Upon electronic excitation a softening of the C–C stretch and a stiffening of the C–N stretch has been observed [2,10]. The situation is depicted in figs. 1a and 1b respectively. The vertical dashed lines represent transitions for a molecule where one of the ^{12}C (or ^{14}N) is replaced by the heavier isotope. In fig. 1a the result is a blue-shift and in fig. 1b a red-shift.

For a single excited vibration, e.g. 6_0^1, one has to add the effect of the isotopic substitution for this particular mode to obtain the observed isotopic shifts ($\Delta^{13}C$ and $\Delta^{15}N$), see table 3.

4. Analysis

In table 3 the measured rovibronic transitions are summarized with their relative experimental uncertainty. Band origins are listed with respect to the 0_0^0 transition and the type of transition is indicated; Q indicates a quadrupole transition. Bands represented in a separate figure are also indicated.

Final levels of different symmetry can be accessed by using one- and two-photon excitation and since the laser source is of high brightness even quadrupole transitions become observable.

Fig. 2 displays the experimental result for the 0_0^0 band. The two-photon 0_0^0 spectrum is displayed in fig. 2a, whereas the 0_0^0 quadrupole transition is shown in fig. 2b. The most intense features in the two-photon spectrum represent the unresolved Q-branch; the width (fwhm about 1 GHz) is mainly Doppler limited. In section 3 the relative strength of this branch with respect to the $\Delta J \neq 0$ bands is briefly discussed,

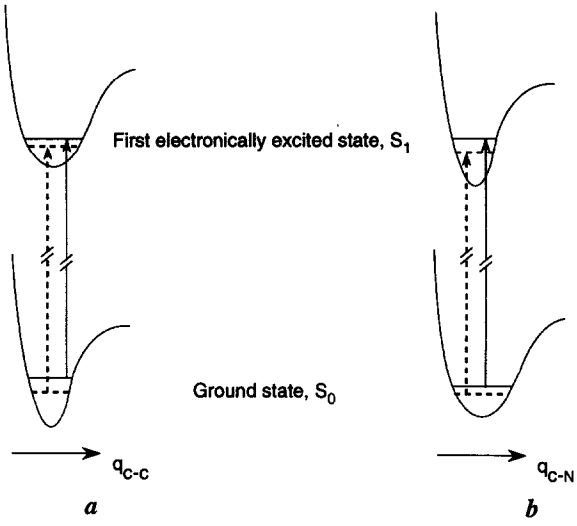

Fig. 1. A qualitative potential for a dominant C–C stretching mode is shown in (a). The full lines correspond to DABCO with six ^{12}C atoms, the dashed ones to the molecule with one ^{12}C atom substituted by a ^{13}C (natural abundance 6.6%). The potential well in the S_1 state is more shallow, in agreement with the observation of a red-shift upon electronic excitation [1,2]. The isotopic shift is to the blue (vertical dashed line) with respect to the most abundant isotopomer. The situation depicted in (b), corresponding to a potential for a dominant C–N stretch, is reversed with respect to case (a), see refs. [1,2]; therefore a red-shift results from a ^{15}N substitution (natural abundance 0.8%).

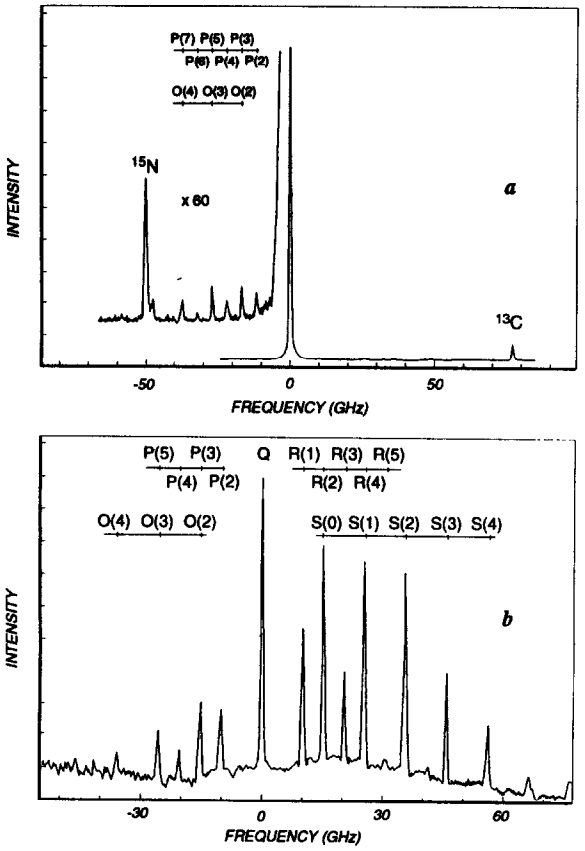

Fig. 2. The LIF spectrum for the 0_0^0 band. In (a) the two-photon 0_0^0 transition is depicted; three Q branches are visible; the two weak ones, blue- and red-shifted, are due to isotopomers. The zero-point energy of all modes is responsible for isotopes shift. Upon substitution $^{12}C \rightarrow {}^{13}C$ ($^{14}N \rightarrow {}^{15}N$) the main change occurs in the C–C (C–N) stretching coordinate. The one-photon 0_0^0 transition is reported in (b); the intensity alternation and the absence of the lines adjacent to the band origin are typical of a quadrupole transition, see text.

for one-photon quadrupole and two-photon transitions. The low rotational temperature allows observation of rotational levels up to $J=5$. From the rotational structure the rotational constants B'' and ΔB are derived, see table 2. The width of the $\Delta J \neq 0$ transitions is comparable to that of the Q-branch. The expected intensity alternation between even and uneven J values characterizing the P and R branches is about one to two for low J values, see section 3. In the two-photon spectrum, fig. 2a, the Q-branches of different isotopomers are visible. Replacing one of the C-atoms by ^{13}C caused an isotope shift $\Delta C = 2.535$ cm^{-1} with an intensity drop to 6.6%. For the ^{15}N isotopomer a red shift of $\Delta N = -1.571$ cm^{-1} is observed with an intensity drop to 0.8%. Two additional Q-branches of isotopomers are observed shifted by 1.605 cm^{-1} and 1.893 cm^{-1} with intensities of 0.06% and 0.18%, respectively, see table 3. The shift of the isotopomer's Q-branches points to a dominant contribution from the C–C (C–N) stretch for the $^{13}C(^{15}N)$ isotopomer, see section 3.

In table 3 three two-photon transitions to fundamentals of a_1' symmetry are shown, the ν_6' band at 671 cm^{-1}, ν_5' band at 778 cm^{-1} and the ν_4' band at 882 cm^{-1}. The latter two are also found as one-photon quadrupole transitions. These assignments are new for what concerns ν_5' and ν_6' and are based on the assumption that the order of increasing energy does not change upon electronic excitation, taking the ν_4' band as listed in reference [1,2].

In addition table 3 contains four two-photon tran-

sitions leading to overtone and combination bands of a_1' symmetry. Naturally, their assignments are rather uncertain, especially because they may be also of mixed character like the a_1' bands at 897 cm^{-1} and 901.1 cm^{-1}.

Four one-photon transitions to excited fundamentals of e′ symmetry are listed in table 3, the ν_{27}' band at 449 cm^{-1}, the ν_{26}' band at 825 cm^{-1}, the ν_{25}' band at 900.5 cm^{-1} and the ν_{24}' band at 1011 cm^{-1}. Except for the ν_{25}' band, these assignments are in agreement with previous ones [1,2]. If one compares the two perpendicular bands, ν_{27}' fig. 3a and ν_{26}' fig. 3b, one notices that the two rotational structures look dissimilar, though belonging to the same band type. In the figure three groups of lines are indicated which have the same rotational assignment. Since one deals with transitions taking place between a nondegenerate ground state, and a degenerate level, the Coriolis coupling has to be taken into account in the expression for the transition energy. Based on the fit of the experimental data it has been concluded that the Coriolis coupling ζ undergoes a 30% variation, see table 2, affecting the separation between successive rotational lines belonging to different K values for the two perpendicular transitions, ν_{26}' and ν_{27}'.

For an overtone transition $2' \leftarrow 0''$, with the fundamental of e′ or e″ symmetry, the final level has two possible symmetries (a_1' and e′) as shown in table 1. Therefore, both the one- and two-photon spectra contain correlated information for this class of transitions: the level of a_1' symmetry can be reached by two-photon excitation, the e′ component by one-photon. The relative energies are slightly different, in general. In table 3 we encounter an example for such a behavior. The band at 897 cm^{-1} ($2\nu_{27}$) behaves regularly having a parallel signature for the two-photon spectrum, and a perpendicular signature for the one-photon spectrum. The two origins are relatively shifted by less than 0.005 cm^{-1}.

New are the two assignments of transitions leading to the excitation of vibrations with final a_2'' symmetry, the combination hot band at 690 cm^{-1} and the ν_{17}' band at 919 cm^{-1}. These are one-photon parallel transitions, the latter being reassigned. Previously the ν_{25}' band of e′ symmetry was thought to be responsible for the band at 919 cm^{-1}. However, the high-resolution results of this work not only yield a much more precise value for the band origin, but demand a parallel band assignment. The one-photon transition at 690 cm^{-1} yields a B'' constant which is off by about 40 MHz from the other B'' values. This is clearly a hot band transition. We suggest that it involves the lowest energy mode, ν_{13}, and a possible combination band with final symmetry a_2'' is $9_0^1 13_1^0$, yielding a value for ν_9' of ≈ 750 cm^{-1}. In addition there are two weak one-photon parallel bands at 671 cm^{-1} and 883 cm^{-1}; suggested assignments as combination bands are given in table 3.

The two bands at 204 cm^{-1} and at 206 cm^{-1} are

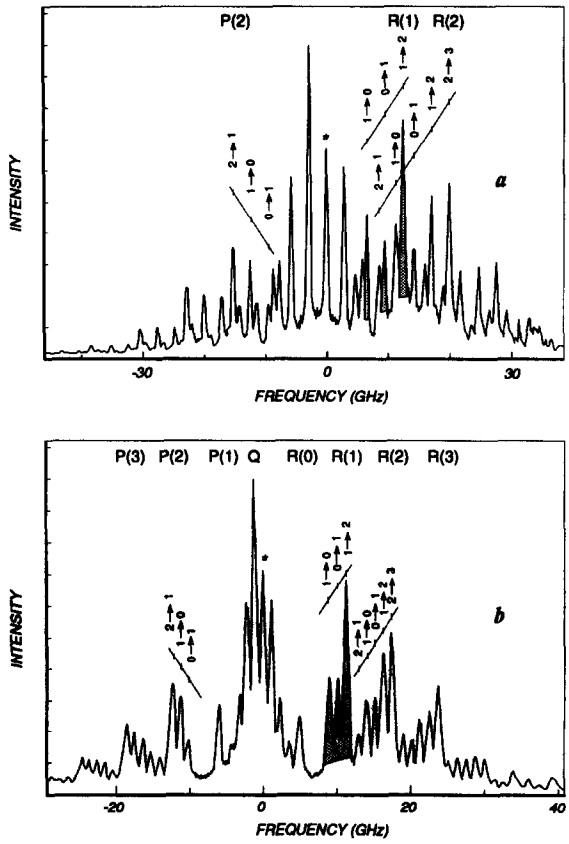

Fig. 3. LIF spectra recorded with one-photon excitation. In (a) and (b) two one-photon perpendicular transitions are reported, ν_{27}' and ν_{26}', respectively. Some rotational identifications J'', K'', ΔJ and ΔK are indicated. The starred lines are assigned as $J''=J'=1$–6, $K''=0\rightarrow1$. The grey shaded lines correspond to $J''=1\rightarrow2$ with, from left to right, $K''=1\rightarrow0$, $K''=0\rightarrow1$, $K''=1\rightarrow2$. The Coriolis coupling is responsible for the bunch of lines having a different spacing in the two ⊥ transitions for the $A'(1-\zeta)$ value; a 30% change has been found between (a) and (b), see text.

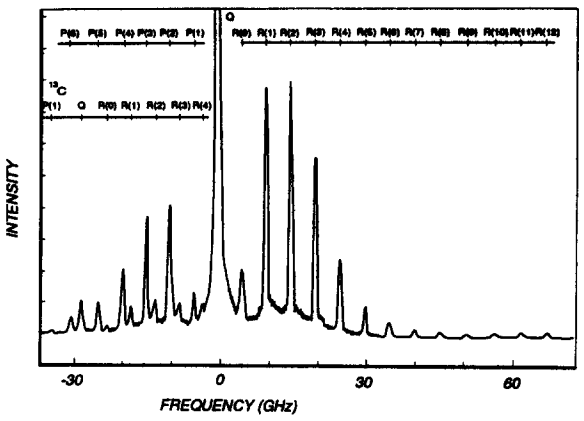

Fig. 4. The ν'_{17} one-photon parallel transition is reported. Note the assigned transitions of the ^{13}C isotopomer.

difficult to assign. We propose for the two-photon transition at 204 cm^{-1} the torsional overtone $2\nu_{13}$ (a'_1)←0′. The other bands remain unexplained so far (see table 3).

The isotope shifts observed for ν'_6 and ν'_{17} bands can be considered with respect to the shifts of the 0^0_0 band, i.e.:

$$\Delta\,^{15}N(\nu'_{17}) - \Delta\,^{15}N(0^0_0) = 0.626\ cm^{-1},$$

$$\Delta\,^{13}C(\nu'_{17}) - \Delta\,^{13}C(0^0_0) = -4.426\ cm^{-1},$$

$$\Delta\,^{15}N(\nu'_6) - \Delta\,^{15}N(0^0_0) = -0.061\ cm^{-1},$$

$$\Delta\,^{13}C(\nu'_6) - \Delta\,^{13}C(0^0_0) = -4.024\ cm^{-1}.$$

A cautious conclusion about these differences may be that for both fundamentals the C–N stretch motion is important, with little displacement of the N-atoms.

Table 2 shows that the changes of rotational constants upon electronic excitation are within our experimental accuracy and do not reflect a large variation in geometry upon electronic excitation.

5. Discussion

In the analysis of single vibrational level dispersed fluorescence (SVL) spectra previously reported [11] three categories of decay have been identified for one-photon excitation. Category 1 consists of transitions without memory effect, i.e. final state after fluorescence decay does not contain a vibrational excitation corresponding to the one excited in the S_1 state. These are simply $S_1(e')\rightarrow S_0(a'_1)$ bands. Category 2, however, leads to a final state where the excited vibration of the S_1 state, e.g. of e′ symmetry, is found back combined with other vibrations, again of e′ symmetry to yield the proper total final symmetry, a'_1 symmetry. Category 3 corresponds to a situation very similar to that of category 2; however, extra excitation of a'_1 symmetry is also seen in the final state. The low-resolution spectra were recorded for excitation energies containing vibrations assumed to be of e′ symmetry [10]. Based on this analysis a correspondence has been determined between ground state and excited state vibrational frequencies [10]. The high-resolution spectra, measured in our laboratory with one and two-photon excitation, shed new light on those results. For three of the four bands we could confirm the previous assignments. In D_{3h} one-photon excitation allows access to levels of e′-symmetry (perpendicular transitions) and to levels of a''_2 symmetry (parallel transitions). The fourth band, at 919 cm^{-1}, measured with high resolution in the present study, could only be assigned as a state of a''_2 symmetry.

The presence of parallel transitions, i.e. the observation of transitions to states of a''_2 symmetry in the one-photon spectrum of DABCO, including the band at 919 cm^{-1}, previously assigned as ν'_{25}, leads to the question of position and identity of the coupling with a state of A''_2 electronic symmetry.

There are two approaches in the literature to the electronically excited states of DABCO. Most often [12–14] the symmetric and anti-symmetric combination of the lone pair orbitals in the ground state $n(+)$ and $n(-)$ is simply extended to the excited state Rydberg orbitals, yielding for $n=3$ the $3s(+)(A'_1)$, $3s(-)(A''_2)$, $3p_{xy}(+)(E')$, $3p_{xy}(-)(E'')$, $3p_z(+)(A''_1)$ and $3p_z(-)(A''_2)$ excited states. As pointed out by Robin [15], however, this always yields more excited state orbitals than can be accounted for spectroscopically. These observations are based on a wide series of "double" molecules, especially the diones. Robin suggests that Rydberg states even of double (two identical chromophores) molecules should be molecule-centered, yielding for DABCO only the $3s(A'_1)$, $3p_{xy}(E')$, $3p_z(A''_2)$ $n=3$ states. This single center approach appears to be nicely confirmed in DABCU (diazabicyclo[3,3,3] undecane) [5], the next larger caged amine, where tran-

sitions from $n(-) \rightarrow 3s$, $3p_{xy}$ and $3p_z$ are assigned by comparing the one- and two-photon spectra. The 3s and $3p_{xy}$ states of DABCO have been assigned as S_1 (A_1') at 35783 cm^{-1} and S_2 (E') at 39814 cm^{-1}, respectively. Thus far there is no direct evidence for the $3p_z$ state which, by analogy with NH_3 [16] and ABCO [17], and by ab initio MO theory [12], is expected to lie slightly higher than the $3p_{xy}$ state. Ito and coworkers [1] have observed three optically active Rydberg series in DABCO with quantum defects $\delta=0.05$, $\delta=0.19$ and $\delta=0.45$ which can be assigned to d, p_z and p_{xy}, respectively [15]. The p_z series is extrapolated to have its lowest ($n=3$) component, lying 2000 cm^{-1} higher than the $3p_{xy}$ component. Avouris and Rossi [12] calculated that the oscillator strength for $3p_z$ is lower than for the $3p_{xy}$ for the corresponding states in ABCO. Based on these qualitative facts we suggest that the electronic state responsible for the a_2'' vibrational coupling in DABCO is the $3p_z$ component which underlies stronger and unresolved vibrational bands of the $3p_{xy}$ transition.

To reconcile the SVL result with the new assignment of the 919 cm^{-1} band the memory effect has to be revisited. The first step consists in writing a proper wavefunction to characterize the electronic states involved in the process. In what follows the rotational contribution to the wavefunction will be neglected because we discuss the memory effect for low-resolution SVL measurements. The symmetry of the states involved plays an important role as selection rules restrict the allowed transitions.

After fluorescence the final ground state wavefunction can be written to describe the memory effect

$$\Psi_f = |S_0(A_1'),\ [n_{\rho 1}\nu''_{\rho 1}(a_2'') + n_{\sigma 1}\nu''_{\sigma 1}(e') + n_{\tau 1}\nu''_{\tau 1}(a_1')]\rangle . \quad (4)$$

The possible final states form a much larger manifold than what is described by eq. (4). We have selected those which were mainly observed in the SVL spectra and which are needed in the following discussion. The n values are mostly 0 or 1; the combination of the vibrations is assumed to be of e'' symmetry since the overall symmetry after fluorescence decay should be E'', $a_2'' \otimes E' = E''$ in D_{3h}.

The $S_1 \leftarrow S_0$ transition is forbidden since both the electronic states have A_1' symmetry in D_{3h}. The $S_2 \leftarrow S_0$ transition is allowed, for perpendicular excitation, because the second electronic state at 250 nm has E' symmetry, and the $S_3 \leftarrow S_0$ transition is allowed, for parallel excitation, assuming this higher electronic state of A_2'' symmetry.

To properly describe the decay process the excited state wavefunction has to involve the S_1, S_2 and S_3 electronically excited states. The initial wavefunction of total A_2'' symmetry can be written as

$$\Psi_i = \alpha|S_1(A_1'),\ n_{\rho 2}\nu'_{\rho 2}(a_2'')\rangle + \beta|S_2(E'),\ [n_{\rho 3}\nu_{\rho e}(a_2'') + n_{\sigma 2}\nu_{\sigma 2}(e') + n_{\tau 2}\nu_{\tau 2}(a_1')]\rangle + \gamma|S_3(A_2''),\ n_{\tau 3}\nu_{\tau 3}(a_1')\rangle . \quad (5)$$

In eq. (5) the combination $n_{\rho 3}\nu_{\rho 3}(a_2'') + n_{\sigma 2}\nu_{\sigma 2}(e') + n_{\tau 2}\nu_{\tau 2}(a_1')$ is of total e'' symmetry.

The initial vibrational state, $\nu'_{\rho 2}$, is due to a parallel excitation with the transition dipole moment, $\hat{O}_{dip}(A_2'')$, along the z direction.

We assume the main transition dipole moment for the decay, $\hat{O}_{dip}(E')$, to lie in the x, y plane. The decay probability (DP) obeys then

$$DP \propto |\langle \Psi_f | \hat{O}_{dip}(E') | \Psi_i \rangle|^2 . \quad (6)$$

To discuss the memory effect we consider explicitly

$$DP \propto \beta^2 |\langle S_0(A_1') | \hat{O}_{dip}(E') | S_2(E') \rangle \times \langle n_{\rho 1}\nu''_{\rho 1}(a_2'') + n_{\sigma 1}\nu''_{\sigma 1}(e') + n_{\tau 1}(a_1') | n_{\rho 3}\nu_{\rho 3}(a_2'') + n_{\sigma 2}\nu_{\sigma 2}(e') + n_{\tau 2}\nu_{\tau 2}(a_1')\rangle|^2 . \quad (7)$$

We have assumed that the dipole operator $\hat{O}_{dip}$ acts only on the electronic coordinates of the molecule. Therefore, in eq. (5) the first and the third term do not contribute to the matrix element of eq. (7).

Before we enter into the discussion of DP we have to consider the mixture of S_1, S_2 and S_3 states in eq. (5). This mixture is a consequence of a term $\hat{H}_{mix}$ in the Hamiltonian, of A_1' symmetry, that couples electronically the S_1, S_2 and S_3 states and simultaneously the indicated vibrational modes $\nu_{\rho i}$, $\nu_{\sigma i}$ and $\nu_{\tau j}$. To couple the three electronically excited states of eq. (5) two $\hat{H}_{mix}$ operators are needed both of the form qQ,

$$\hat{H}_{mix\,\rho} \propto q(A_2'')Q_{\rho 2}(a_2'') \quad (8)$$

and

$$\hat{H}_{mix\,\sigma} \propto q(E')Q_{\sigma 2}(e') . \quad (9)$$

Here Q stands for a normal coordinate of a vibrational mode and q for an electronic coordinate. These

terms are of the second order in the coordinates, in simplest possible case. If $n_{\tau 2}$ is not assumed to be zero in eq. (5) a third-order $\hat{H}_{\mathrm{mix}}$ is required.

To discuss DP we first assume $n_{\rho 1}=n_{\sigma 1}=n_{\rho 3}=n_{\sigma 2}=1$ and $n_{\tau 1}=n_{\tau 2}=n_{\tau 3}=0$, with $\rho 1=\rho 3$ and $\sigma 1=\sigma 2$. These decay channels have been observed and are defined as category 2 transitions, see ref. [10].

Alternatively, we are led to category 3 transitions if we put $n_{\tau 3}=0$ and $n_{\rho 1}=n_{\sigma 1}=n_{\tau 1}=n_{\rho 3}=n_{\sigma 2}=n_{\tau 2}=1$.

For category 1 decay there is no "memory effect"; since this channel has also been observed we will discuss it in the following. To this aim eq. (6) is replaced by

$$\mathrm{DP}\propto|\langle\Psi_{\mathrm{f}}|\hat{O}_{\mathrm{dip}}(\mathrm{A}_2'')|\Psi_{\mathrm{i}}\rangle|^2 . \tag{10}$$

Explicitly

$$\mathrm{DP}\propto\gamma^2|\langle\mathrm{S}_0(\mathrm{A}_1')|\hat{O}_{\mathrm{dip}}(\mathrm{A}_2'')|S_3(\mathrm{A}_2'')\rangle \times\langle n_{\tau 1}\nu_{\tau 1}''(\mathrm{a}_1')|n_{\tau 3}\nu_{\tau 3}(\mathrm{a}_1')\rangle|^2 . \tag{11}$$

We have again assumed that the dipole operator $\hat{O}_{\mathrm{dip}}$ acts only on the electronic coordinates of the molecule. Therefore, in eq. (5) the first and the second term do not contribute to the matrix element of eq. (7). To couple the three electronically excited states of eq. (5) a third-order $\hat{H}_{\mathrm{mix}}$ operator is needed

$$\hat{H}_{\mathrm{mix},\rho\tau}\propto q(\mathrm{A}_2'')Q_{\rho 2}(\mathrm{a}_2'')Q_{\tau 3}(\mathrm{a}_1') . \tag{12}$$

One has $\tau 1=\tau 3$ with $n_{\tau 1}=n_{\tau 3}=1$ and $n_{\rho 1}=n_{\sigma 3}=0$.

In this way we have demonstrated that the "memory effect" holds also for parallel excitation and yields a similar SVL spectrum as for perpendicular transitions. The band at 919 cm^{-1} can thus be assigned as ν_{17}' of a_2'' symmetry. Based on this assignment the SVL data yield for the ground state ν_{17}'' the value 986 cm^{-1}. This result is in agreement with the findings of previous investigations [2,10].

6. Conclusions

Analysis of rotational structure in vibronic transitions is well known to yield a wealth of information on molecular properties, particularly on vibrational mode symmetry and molecular geometry. In this paper it is shown that this is also true for a 20 atom molecule such as DABCO, given sufficiently low rotational temperatures and narrow laser bandwidths. Table 3 contains an overview of information obtained on the $S_1\leftarrow S_0$ transition of DABCO.

Two different measurements, isotope shifts and rotational constants, provide information on the structural changes taking place on excitation to the S_1 electronic state. Changes in the overall shape of the molecule are reflected by the rotational constants. Although it was not possible to individually extract A'' and A' from the spectra, from the analysis it is clear that ΔA is small, less than 0.1% of A''. The molecule thus becomes very slightly more prolate in S_1. From the isotope shifts measured for the 0_0^0 band the tightening of C–N bonds and weakening of C–C bonds is confirmed by a blue-shift for the ^{13}C isotope and a red-shift for the ^{15}N isotope. Interestingly, this shift for the ^{13}C isotope changes sign for the two excited vibrational levels (ν_6' and ν_{17}') where also isotope shifts were observed. The long progression seen for the ν_5 and for the ν_3 vibrational modes of the $S_1\leftarrow S_0$ transition indicate that geometry changes do take place. On excitation to the ion-like 3d Rydberg state (S_1) electron density is seen to move out of the C–C bonds and into the C–N (and N–N) bonds, just as predicted by Heilbronner and Muskat [18] for $n(+)\rightarrow$ ion transitions. Overall, these changes have little effect on the rotational constants, suggesting that the C–N–C angle opens up enough to compensate for longer C–C distances, yielding almost the same rotational constants for S_1 as for S_0.

Assignments of vibrational mode symmetries is aided by the rotational analysis. For instance the reassignment of the strong 919 cm^{-1} band as of a_2'' symmetry indicates that coupling through an A_2'' electronic state, possibly the unassigned $3p_z$ Rydberg state, is also significant in DABCO.

References

[1] N. Gonohe, N. Yatsuda, N. Mikami and M. Ito, Bull. Chem. Soc. Japan 55 (1982) 2796.
[2] D. Consalvo, J. Oomens, D.H. Parker and J. Reuss, Chem. Phys. 163 (1992) 223.
[3] P. Bishof, J.A. Hashmal, E. Heilbronner and V. Hornung, Tetrahedron Letters (1969) 4025.
[4] P. Bruësch, Spectrochim. Acta 22 (1966) 861.
[5] K. Ray, M.A. Quesada and D.H. Parker, J. Phys. Chem. 92 (1988) 5436.

[6] H. Zuckermann, Y. Haas, M. Drabbels, J. Heinze, W.L. Meerts, J. Reuss and J. van Bladel, Chem. Phys. 163 (1992) 193.
[7] G. v.d. Hoek, D. Consalvo, D.H. Parker and J. Reuss, Z. Physik D 27 (1993) 73.
[8] K.-M. Chen and E.S. Yeung, J. Chem. Phys. 69 (1978) 43.
[9] G. Herzberg, in: Molecular spectra and molecular structure, Vol. 3 (Krieger, New York, 1991) pp. 226, 232.
[10] D. Consalvo, D.H. Parker and J. Reuss, Chem. Phys. 165 (1992) 397.
[11] M. Fujii, private communication.
[12] P. Avouris and A.R. Rossi, J. Phys. Chem. 85 (1981) 2340.
[13] M.A. Smith, J.W. Hager and S.C. Wallace, J. Phys. Chem. 88 (1984) 2250.
[14] G.J. Fisanick, T.S. Eichelberger, M.B. Robin and N.A. Kuebler, J. Phys. Chem. 87 (1983) 2240.
[15] M.B. Robin, in: Higher excited states of polyatomic molecules, Vols. 1, 2 (Academic Press, New York, 1974), Higher excited states of polyatomic molecules, Vol. 3 (Academic Press, New York, 1985).
[16] J.H. Glownia, S.J. Riley, S.D. Colson and G.C. Nieman, J. Chem. Phys. 73 (1980) 4296.
[17] A.M. Weber, A. Acharya and D.H. Parker, J. Phys. Chem. 88 (1984) 6087.
[18] E. Heilbronner and K.A. Muskat, J. Am. Chem. Soc. 92 (1970) 3818.